Biophysical Chemistry 4 (1976) 171–179

EQUILIBRIUM GEL PERMEATION: A SINGLE-PHOTON COUNTING SPECTROPHOTOMETER FOR STUDIES OF PROTEIN INTERACTION *

Gary K. ACKERS, Erich E. BRUMBAUGH, Stephen H.C. IP and Herbert R. HALVORSON
Department of Biochemistry, University of Virginia, Charlottesville, Virginia 22901, USA

Received 14 November 1975

When a small column or flow cell packed with gel particles is completely saturated with a solution containing molecular species of interest, the average cross-sectional area occupied by the solute (partition cross section) is conveniently and precisely determined by direct optical scanning. For a mixture of interacting solutes this equilibrium gel permeation measurement yields the weight average of the species partition cross sections and the variation of this quantity with solute concentration permits determination of the solute interaction parameters (stoichiometry, equilibrium constants). We have developed a computer-controlled single-photon counting spectrophotometer for these measurements. The instrument exhibits high precision over a wide range of optical density. With counting times in the range of 10–1000 s the standard deviations on optical densities of protein solutions measured at 220 nm are typically 0.0006 at 1 OD, 0.002 at 2 OD, 0.005 at 4 OD. Beer's law tests show that deviations from linearity are less than these precision limits. Partition cross-section measurements for proteins can be made with an accuracy of better than 0.001 and information can be obtained with protein solutions at least as low as 1 μg/ml.

1. Introduction

Interactions between subunits of biological macromolecules are well-known to play major roles in the self-regulation of functional complexes such as enzymes, respiratory carriers, immunochemical and mechanochemical systems. Studies of reversible subunit interaction thus provide vital information regarding mechanisms of stability and self-assembly in such systems. They also provide a powerful means of probing intersubunit contact energy changes which accompany such processes as cooperative ligand binding.

Characterization of reversibly self-associating solutes must logically begin with a determination of which polymer species are present under various conditions of interest, and in what proportions. The problem of unambiguously determining the species distribution in even a simple (two or three species) self-associating equilibrium is not a simple task. Much effort in recent years has been devoted to developing experimental techniques and numerical methods which would make such analyses routine. However the degree of success that has been achieved toward this goal has generally been less than spectacular so that new developments are of continuing interest.

Interacting solutes, such as self-associating proteins or protein–ligand mixtures, are frequently characterized by studying a weight-average molecular property under varying solution conditions. The degree of solute permeation within an inert porous gel provides a convenient and sensitive means of studying molecular size properties in such systems (cf. refs. [1,2]). These properties can be utilized either in transport experiments (gel chromatography) [3–12] or in purely equilibrium experiments (equilibrium gel permeation) [13–15]. Molecular size-dependent partition coefficients may be obtained by either approach. The transport experiments provide additional information contained in the solute profile shapes [4,5,9–12]. Equilibrium gel permeation experiments performed by direct optical scanning of saturated columns have been shown to provide a convenient method for obtaining the relevant equilibrium quantities. Using a scanning

* Supported by Grant GM-14493 from the National Institutes of Health.

gel chromatograph developed in this laboratory [13], the method has been used to explore both single solute protein systems [14] and protein–ligand binding reactions [15].

This paper describes results obtained with a computer-controlled single-photon counting spectrophotometer designed specifically to measure equilibrium gel permeation. Instead of scanning a chromatographic column [13] the new instrument measures optical densities of small flow cells packed with gel particles. In addition to allowing small sample quantities, it also affords considerably higher photometric precision than has previously been obtainable at the necessarily high optical densities encountered in this experimental technique.

The basic measurement consists of determining the optical density of a bed of close-packed gel particles (e.g. Sephadex) at equilibrium with a given solution whose properties are to be studied (i.e., the gel bed has been "saturated" with the solution of interest). Subtracting from this the optical density of the gel bed measured in the absence of solute gives the absorbance, A_b, of solute partitioned within the gel bed. The effects of light scattering and solute absorptivity are completely decoupled in these systems [13]. A corresponding absorbance measurement, A_a, is made of the free solution (i.e., in a cell with no gel) at the same pathlength. The ratio of A_b to A_a then gives the partition cross section ξ representing the fraction of area within the gel bed accessible to solute [13].

$$\xi = \alpha + \beta\sigma. \tag{1}$$

In eq. (1) α and β are the void and internal cross sections, respectively, and σ is the (molecular size-dependent) partition coefficient. If two or more species are present the measured partition cross section is a weight average, $\bar{\xi}_W$, over the species cross sections

$$\bar{\xi}_W = \sum_i f_i \xi_i, \tag{2}$$

where f_i is the weight fraction of species i and ξ_i its partition cross section. A series of such measurements of $\bar{\xi}_W$ as a function of some solution parameter (usually protein concentration or protein–ligand ratio) provides the information necessary to infer stoichiometries and equilibrium constants [4–8,15].

The requirements of this experiment place severe demands upon the accuracy and dynamic range of spectrophotometric performance. This is particularly true when systems are to be studied at very low solute concentration. The optical density of a 0.5 cm pathlength flow cell packed with Sephadex (saturated with transparent solvent) can be as high as 2 OD units at 215 nm. Because of this high baseline the spectrophotometric response must be linear over a wide range. In addition, the accuracy must be high at high optical densities, since information at protein absorbances less than 0.01 is needed for some systems. Thus the spectrophotometer for this experiment must be capable of measuring (a) very low absorbances (A_a at low conc), (b) small differences between large optical densities (OD_b and A_b) and (c) high optical densities and absorbances (at high concentrations). Furthermore, the low protein concentrations which must be employed in many studies require an ability to exploit the high extinction of proteins at low wavelengths (e.g., 210–225 nm); therefore the instrument must meet the above requirements in this low wavelength region. We report here the results of tests which show that our instrument meets these requirements, and thus provides greatly increased capabilities over previous instrumentation.

2. Photon counting spectrophotometer – design and operation

The spectrophotometer we have built employs the technique of single-photon counting. The photon counting technique has proved useful in many areas of photometric measurement, particularly where only low light intensities are available [16,17]. The digital output characteristics of the photomultiplier tube are utilized to obtain a single pulse for each incident photon making a fruitful collision with the photocathode. By optimizing the system for this characteristic one gains the dual advantages of digital data processing with its concomitant error reduction and extension of the measurement range to high optical densities. Compared to analog light measuring systems, photon counting techniques provide greatly improved signal to noise ratio, long-term stability, and linear response over a wide dynamic range.

The optical design of the spectrophotometer is conventional, as shown in fig. 1. The light source is a deuterium lamp powered by a Schoeffel model LPS 301

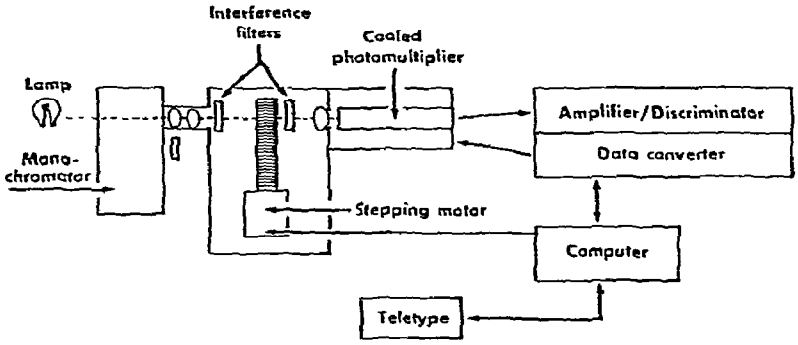

Fig. 1. Diagram of single-photon counting spectrophotometer. The stepping motor mounted in the cell compartment, positions the sample carriage (fig. 2) by means of a precision screw to any of two thousand positions under computer control. The computer determines time constant and total counting time for the photometric system, performs statistical analyses during data acquisition, and can be used to adjust sampling times for optimization of experiments.

power supply operating at 60 watt. Radiation from the source is directed through a Zeiss M4 QIII monochromator, used without the beam chopper. Two custom-made 30 nm bandwidth interference filters (Infrared Industries, Waltham, MA) eliminate stray light (light from wavelengths other than the monochromator setting). The first quartz condensing lens provides a converging beam of light impinging upon the sample. A circular aperture of 1 or 2 mm dia. is placed just before the sample. The second lens collects the light that has passed through the sample and focuses it on the end-window of the photomultiplier tube (EMI 6256SA). A sample carriage (fig. 2) is advanced by a stepping motor turning a precision screw. This cell holder may be placed at any of two thousand positions separated by 25 μm (corresponding to one increment of the stepping motor). The cell positions are reproducible to within a tolerance considerably smaller than a single step. The stepping pulses are generated by a digital computer under control of a crystal clock,

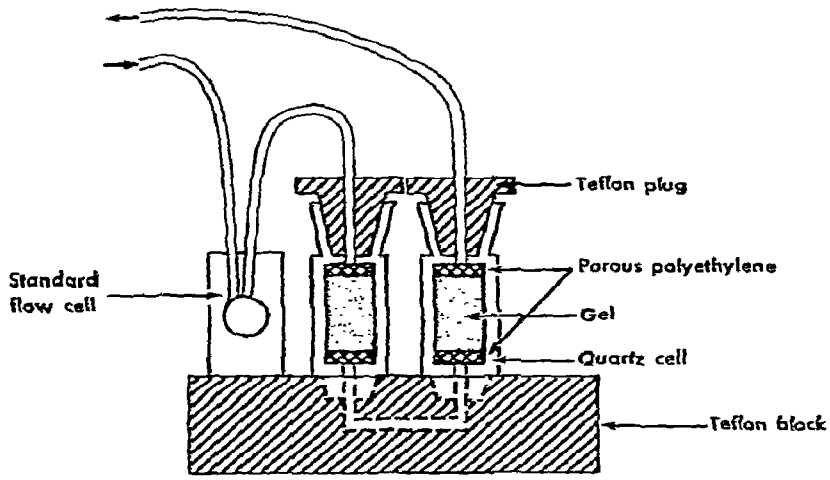

Fig. 2. Side view of sample carriage (diagramatic) showing flow system for gel permeation experiments with two gel cells. When mounted in the instrument the optical beam is perpendicular to the plane of this diagram. The cells are measured in sequence: air reference, first gel cell, second gel cell, standard flow cell. The cell train is first measured when saturated with buffer; then subsequently after saturation (judged by constancy of absorbances in the "last" flow cell of the train) with the protein solution. When the baseline values are subtracted, comparison of protein absorbance in a gel cell with that of the standard flow cell (corrected to the same pathlength) yields the molecular-size-dependent partition cross section directly.

providing great flexibility in positioning sequence and timing. The nominal driving speed is set at 100 steps/s. In most experiments four cells are used in the cell carriage.

The photometric system consists of an EMI 6256SA photomultiplier housed in a cooling chamber (Products for Research model TE-104TS). An amplifier/discriminator (Solid State Radation, model 1120) amplifies and shapes the photomultiplier output pulses into a form suitable for counting by the Data Converter (SSR model 1105). Pulse pair resolution time is 25 nanoseconds. Under control of a crystal clock, the Data Converter counts pulses for a predetermined period of time and stores the accumulated number of events in a 16-bit buffered register. The data are then transferred in parallel into the digital computer (Hewlett Packard 2114A 8K) for processing. The computer also uses a crystal clock for overall timing operations. Upon completing a measurement the computer commands the stepping motor to advance the cell holder to the next cuvet and a new measurement is begun.

The software for the computer permits great flexibility in measurement. The user can preselect arbitrarily located positions for the measurements. For each position there is associated an accumulation time ("time constant"). Since each datum is limited by the output register of the data converter to 16 bits (32K) the individual count is repeated several times by specifying a total measuring time for each position. Typical values are 0.01 s for the time constant and 10 or 100 s for the total time, yielding 1000 and 10000 repeated measurements, respectively. Similar considerations apply for determinations of the dark count which is generally in the range of 2–10 counts/s with the tube cooled to 10°C.

Upon cycling once through all the desired positions, the data are converted from mean counts/s ("intensities") to absorbances. The instrument continues this process for a predetermined number of cycles, prints out the data at each stage, and finishes by printing the mean and standard error of the mean for each measurement. Statistical analyses can also be performed on the raw accumulated data.

An example of a typical measurement sequence is shown in table 1 for a series of 5 sequential measurements of a carriage loaded with four cells. The reference was a sealed cuvet containing buffer. Cells 2 and 3 (0.5 cm pathlength) are flow cells packed with Sephadex gels G-75 and G-100 respectively. Cell 4 is a flow cell (1 cm pathlength) in series with cells 2 and 3 but contains no gel. The flow cells 2, 3 and 4 have been saturated with a solution of carboxyhemoglobin at a concentration of 0.95 μ/moles heme/ℓ. The measurements are made at 215 nm with counting times of 10 s for cells 1 and 4 and 100 s for cells 2 and 3.

Table 1
Typical absorbance measurement sequence

Cycle	Reference[a]	Cell 2[b]	Cell 3[c]	Cell 4[d]
1	5.10106	2.15082	1.74272	0.35580
2	5.10273	2.15079	1.74643	0.35607
3	5.10236	2.15092	1.74523	0.35891
4	5.10259	2.15051	1.74661	0.35886
5	5.10313	2.15395	1.74656	0.36195
Mean	5.10237	2.15140	1.74551	0.35832
Std. Dev.	0.00035	0.00064	0.00074	0.00112

a) The reference position samples air. Numbers here are logarithims of counting rate. All other numbers are in absorbance units.
b) A 0.5 cm pathlength cell packed with Sephadex G-75.
c) A 0.5 cm pathlength cell packed with Sephadex G-100.
d) A 1.0 cm pathlength flow cell containing no gel. Cells 2, 3, and 4 have been saturated with a solution of carboxyhemoglobin at a concentration of 0.95 μM heme/ℓ. Measurements are at 215 nm. Counting times were 10 s for cells 1 and 4, 100 s for cells 2 and 3.

3. Experimental methods and results

3.1. Materials

Sephadex G-100 (Pharmacia lot 6164) and G-200 (lot 7884) were used for the experiments described in this paper. An LKB Perpex pump was used to maintain a flow rate of 3.6 ml/hr. Sperm whale myoglobin was obtained from Sigma Chemical Company. Ovalbumin, aldolase, chymotrypsinogen A and ribonuclease A were from Pharmacia (calibration kit). Glycylglycine was from Mann. Gamma globulin was from Miles Turnip Yellow Mosaic virus was a gift from Dr. W. Godschalk. Buffers were made using EDTA (Sigma lot 61C-9100) and Tris (ultra pure Schwartz/Mann lot #1481).

3.2. Precision and stability of the photometric system

In this section we describe results of incident intensity tests carried out in the absence of samples. These were prerequisite to the subsequent absorbance determinations. First we summarize relationships between the principal factors which define precision and stability in the system.

3.2.1. Basic relationships

Once a suitable tube temperature (generally 5–10°C in this system) and dynode voltage have been found for the photomultiplier (1600 volt) the noise in the instrument is determined by two factors: the inherent uncertainty arising from counting statistics and, more importantly, noise in the light source.

For all practical purposes photons arrive at the photocathode completely independently of one another (although black-body radiation obeys Bose–Einstein statistics, no appreciable error is introduced by the assumption of Boltzmann statistics). Within this approximation the number of photons n arriving in time t described by a Poisson distribution and the standard deviation is just the square root of the mean. For the large numbers involved here we can equate the Poisson distribution with a gaussian ("normal") distribution having mean n and standard deviation $\sqrt{n}$. The measurement n_m is the sum of the signal n_s and the dark count n_d; $n_s = n_m - n_d$. The quantity of major interest is not the number of counts but the rate r at which they occur.

$$n \pm \sqrt{n} = rt \pm \sqrt{rt}\,. \tag{3}$$

The standard error of the rate is

$$\Delta r = \pm\sqrt{r/t}\,. \tag{4}$$

Since the measurement rate and the dark rate are determined in separate experiments, the signal rate and its associated error are (cf. ref. [20]):

$$r_s = (r_m - r_d) \pm \sqrt{(r_s + r_d)/t_m + r_d/t_d}\,. \tag{5}$$

This expression defines the theoretical limit to the precision of a photon-counting measurement.

For the pulse pair resolution of 25 ns characteristic of this instrument there can be appreciable coincident counts at the upper limit counting ranges of 10^7 photons/s. In a series of tests it was found empirically that measured absorbances were independent of incident intensity for incidence rates less than or equal to 5×10^5 photons/s. Consequently this setting was used for all measurements reported.

3.2.2. Incident intensity tests

The stability of a single-beam photometer primarily depends upon the stability of the light source. The best available light source for our purposes has been a deuterium lamp. For a series of 10 s to 100 s runs spaced evenly over a period of one to two hours, the standard deviation was typically around 0.05% to 1%, depending upon the condition of the lamp (at an intensity of 5×10^5 counts/s). This is slightly higher than the theoretical value calculated by the square root method; thus, at present, the light source appears to be the limiting factor in counting uncertainties. For relatively short counting sequences the type of results shown in table 1 (reference position) are typical.

3.2.3. Precision in absorbance measurements

Having established the quality of individual measurements (intensities), we then investigated the uncertainty of calculated absorbances, A,

$$A = \log(R_r/R_s), \tag{6}$$

where r and s refer to reference and sample measurements respectively. The standard error ΔA, in A is given by

$$\Delta A = \frac{1}{2.303}\left\{\frac{1}{R_r t_r}\left[1 + \frac{R_d}{R_r}\left(\frac{t_r}{1+t_d}\right)\right] + \frac{1}{R_s t_s}\left[1 + \frac{R_d}{R_s}\left(\frac{t_s}{1+t_d}\right)\right]\right\}^{1/2}. \tag{7}$$

The relative error $(\Delta A/A)$ is shown in fig. 3 for representative sets of parameters. For comparison, fig. 3 also contains the relative error curve for an analog photometric measurement. It assumes a reference signal of 1 volt and an error of ±0.5 mV in any reading, and is calculated according to:

$$A = \log(I_r/I_s), \tag{8}$$

$$\Delta A = \frac{1}{2.303}\,\frac{\Delta I}{I_r}\,\sqrt{1 + 10^{2A}}\,. \tag{9}$$

This error curve shown in fig. 3 for the analog system corresponds approximately to the performance of our

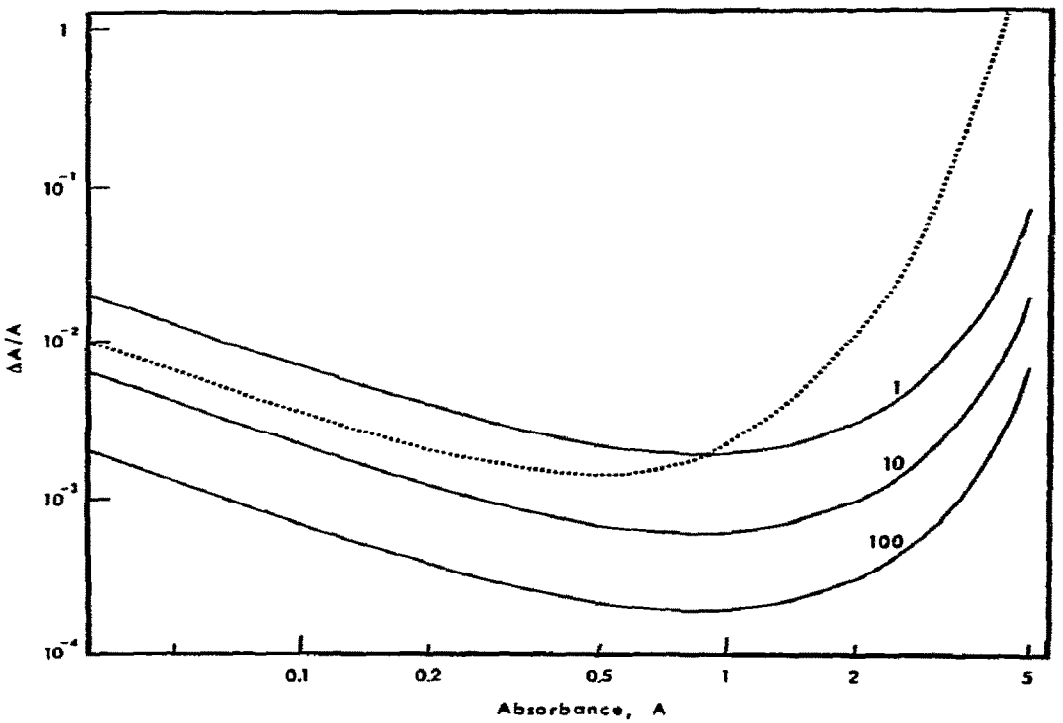

Fig. 3. Error in measured absorbance for photon counting (solid lines) and analog (dashed line) photometric systems. The different solid curves pertain to counting times of 1, 10 and 100 s (see text).

analog gel scanning system previously described [13].

3.3. Measurements with gel partitioning systems

3.3.1. Quality of absorbance measurements

A number of experiments were carried out to determine the stability of absorbance measurements made over long time periods with actual gel partitioning systems. Based on 10 and 100 s runs, the standard deviations of ten individual runs spaced evenly in one and two hour periods are shown in table 2. For these measurements two sample cells were used. One was packed with Sephadex G-100 and the other contained no gel. The first three measurements pertain to myoglobin solutions in the non-gel-containing cell and the others are optical densities of gel bed plus various saturating solutions of myoglobin. Measurements were made at 220 nm. The stability of the optical density measurements over a period of 15 hours. (inside the gel) was found to be very high: the standard error of the mean deviation over the 15 hours, (90 measurements of 100 s each) was 0.0006 at an optical density

Table 2
Error in absorbance measurement

Absorbance	Standard deviation[a)]	Percent error
0.1880	0.00062	0.330
1.1819	0.00052	0.044
1.5245	0.0074	0.049
1.9610	0.0020	0.102
2.4653	0.0025	0.101
3.0174	0.002	0.073
4.0374	0.0048	0.119

Measurements were made at 220 nm using two cells (1) a reference solution cell (0.5 cm pathlength) and (2) a similar cell packed with Sephadex G-100 (also 0.5 cm pathlength). Absorbances are for solutions of myoglobin in these cells. Cell (1) was used to determine the first 3 values and cell (2) for the remainder.

a) Based on 10 runs spaced evenly over a two hour period.

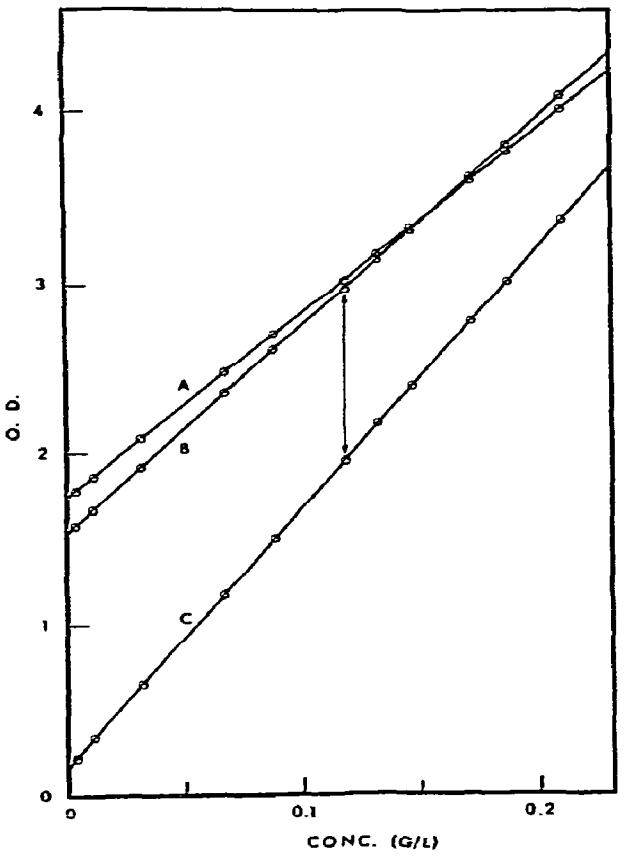

Fig. 4. Beer's law plots for myoglobin at 220 nm. Curve (A): Sephadex G-75; (B): Sephadex G-100; (C): Solution reference cell. Optical densities were measured relative to air reference.

of 2.55. Even though the lamp drifts over this period, the optical density measurement remains essentially constant. Since the gels are optically inhomogeneous, this also tests the reproducibility of the cell positioning and the stability of the gels themselves.

The next step was to assess the quality of the absorbance measurements with respect to linearity and range. An ad hoc test for the presence of stray light is an extended series of Beer's law measurements. If a significant number of uncorrected background counts were present, due either to uncompensated dark count or to stray light, there would be negative deviations from linearity at high absorbances. (We have found empirically that the two interference filters are quite

Table 3
Partition cross sections of proteins[a)]

Solute	G-200 cell	G-100 cell
Glycylglycine	0.9892 ± 0.0009	0.9789 ± 0.0007
Myoglobin	0.7994 ± 0.0005	0.7103 ± 0.0006
Ribonuclease A	0.8231 ± 0.0007	0.7359 ± 0.0008
Chymotrypsinogen A	0.7613 ± 0.0006	0.6632 ± 0.0006
Ovalbumin	0.6418 ± 0.0010	0.5343 ± 0.0009
Aldolase	0.5052 ± 0.0006	0.4058 ± 0.0006
γ-Globulin	0.4593 ± 0.0006	0.3771 ± 0.0010
Turnip Yellow Mosaic Virus	0.3183 ± 0.0007	0.3207 ± 0.0009

[a)] Buffer conditions: 0.05 M TrisHCl, 0.1 M NaCl, mM EDTA, pH 7.6.

effective in eliminating stray light. In combination they eliminate at least six orders of magnitude stray light at remote regions of the spectrum from 220 nm.) Using potassium permanganate solutions of absorbances up to 3.6, no deviation from linearity could be detected. Linear correlation coefficients were 0.99999.

Having demonstrated the capability of measuring absorbance over a wide range, we then addressed problems possibly arising from the gels: Would it be possible to obtain Beer's law plots above the "baseline" optical density of the gel? What would be the effect of light scattered by the gel? Accordingly, we saturated the gels with protein solutions (e.g., myoglobin) and measured optical densities of solution and of gel at 220 nm as a function of concentration (fig. 4). No deviation from linearity was discernible at optical densities of 4.0.

3.3.2. Determination of partition cross sections

Molecular size-dependent partition cross-sections were determined for a number of protein samples in order to assess the accuracy with which such quantities could be determined. The cross sections are shown in table 3 along with error estimates on the values derived. Protein absorbances were generally in the region 0.2–1.0 at 220 nm where measurements were made. The standard deviations were calculated according to the error propagation formula for ξ:

$$\Delta\xi = \frac{1}{2.303A_a}\left\{\left(\frac{\Delta C_{gs}}{C_{gs}}\right)^2 + \left(\frac{\Delta C_g}{C_g}\right)^2 + \xi^2\left[\left(\frac{\Delta C_s}{C_s}\right)^2 + \left(\frac{\Delta C_b}{C_b}\right)^2\right]\right\}^{1/2}, \quad (8)$$

Table 4
Partition cross section of partially liganded hemoblobin[a)]

	Air reference	Gel cell	Solution reference
Counts/s	5.42171×10^5	1.61193×10^4	2.17702×10^5
Error	$\pm 0.00257 \times 10^5$	$\pm 0.00290 \times 10^4$	$\pm 0.00442 \times 10^5$
Optical density	–	1.52679	0.39627
Error	–	±0.00081	±0.00090
Absorbance	–	0.01637	0.05226
Error	–	±0.00228	±0.00162
Partition cross section	–	0.6266	–
Error	–	0.0268	–

a) Hemoglobin solutions were equilibrated with an oxygen–nitrogen mixture prior to flow into the gel. Spectrophotometric analysis after passage through the gel cell and measuring system indicated the sample to be 41% oxyhemoglobin, 51% deoxyhemoglobin, and 8% methemoglobin. The pO_2 was ~5 mm Hg.

where A_a is solution absorbance in the solution reference cell, C_{gs} represents counts of the gel bed plus solute partitioned into it, C_g that of the gel bed alone, C_s is counts of the solution reference cell with protein solution in it and C_b without protein. Reproducibility of partition cross-sections from one experiment to another for the same solute was found to be approximately the same as these error levels (table 3). The accuracy we are achieving is substantially higher than previously achievalbe with the scanning gel chromatograph using analog photometry [14].

In a previous study we have found that the correlation between molecular radius and partition coefficient was at least as good as the precision of 0.0015–0.002 would allow us to calculate when the correlation was made between molecular radii "seen" by two gels of different porosity [14]. As has been shown in previous studies (cf. [8]) the accuracy with which these partition coefficients can be determined over a wide range of conditions, is of great importance in defining the [illegible] of species by numerical analysis of the data.

3.3.3. Studies at the lowest concentration

Determinations of partition cross-section at the lowest concentration are necessarily the most difficult and are subject to the largest errors. In order to explore these limits we carried out experiments with human hemoglobin solutions in a gas-tight system (to be described elsewhere) under conditions of partial oxygenation at low concentration. A representative set of data is shown in table 4 for a solution with an absorbance of 0.052 at 220 nm, corresponding to a concentration of ~2 μg/ml. The error in the determined value of the partition coefficient for this "worst case" example was 0.0268, as compared to the theoretical minimum error (based on counting statistics alone) of 0.008. For solutions with absorbances below 0.05 the error is approximately inversely proportional to the absorbance, predicting a 100% relative error "wipe out" in the range 0.0005 A (theoretical error) to 0.001 A (measured error). This latter corresponds to a hemoglobin solution 5×10^{-9} M in heme or 8×10^{-5} g/l.

4. Discussion

The results obtained clearly show that the single-photon counting instrument provides a higher range of linearity and greater precision in the determination of gel permeation parameters than has previously been available. Subsequent papers will delineate the need for these increased levels of precision in applications to self-associating solutes. The instrument should also have considerable application to the study of macromolecule–ligand binding reactions by the equilibrium saturation method.

The capability of measuring partition cross sections at solute concentrations below one microgram per ml is important for characterization of tightly associated systems [19]. For example, the equilibrium constant for dissociation of unliganded hemoglobin tetramers into dimers has recently been determined to be around 10^{-10} M heme [20]. Happily, meeting the constraints imposed by the low concentration measurements in

the presence of the gel also gives us an instrument capable of working at extremely high concentrations — thus suitable for studying loosely associating systems. We thus believe that the development of this new photon-counting instrument represents a singular advance in the technique of equilibrium gel permeation and, as a consequence, in the field of protein interaction studies.

The equilibrium gel permeation technique, like other equilibrium methods, provides inherently less information than the corresponding nonequilibrium transport methods, but has the advantage of providing data that is vastly more straightforward to analyze. In previous studies [5,9–12] we have explored the sensitivity of reaction profile shapes in gel chromatography to variations in solute parameters as well as parameters of the chromatographic system which are under experimental control. It was shown that such profile shapes inherently contain much information, but that extracting it is a very formidable task. Ideally both equilibrium and nonequilibrium techniques should be used in a complementary fashion in the study of a given unknown system of interest.

References

[1] G.K. Ackers, in: The Proteins, Third Ed., Vol. 1, eds. H. Neurath and R.L. Hill (Academic Press, New York, 1975) p. 1.

[2] D.J. Winzor, in: Physical Principles and Techniques of Protein Chemistry, Part A, ed. S.J. Leach (Academic Press, New York, 1970).

[3] D.J. Winzor and H.A. Scheraga, Biochemistry 2 (1963) 1263.

[4] D.J. Winzor and H.A. Scheraga, J. Phys. Chem. 68 (1964) 338.

[5] G.K. Ackers and T.E. Thompson, Proc. Nat. Acad. Sci. 53 (1965) 342.

[6] G.K. Ackers, J. Biol. Chem. 242 (1967) 3026.

[7] D.J. Winzor, J.P. Loke and L.W. Nichol, J. Phys. Chem. 71 (1967) 4492.

[8] E. Chiancone, L.M. Gilbert, G.A. Gilbert and G.L. Kellett, J. Biol. Chem. 243 (1968) 1212.

[9] J.K. Zimmerman and G.K. Ackers, J. Biol. Chem. 246 (1971) 1078.

[10] J.K. Zimmerman, D.J. Cox and G.K. Ackers, J. Biol. Chem. 246 (1971) 4242.

[11] J.K. Zimmerman and G.K. Ackers, J. Biol. Chem. 246 (1971) 7289.

[12] H.R. Halvorson and G.K. Ackers, J. Biol. Chem. 249 (1974) 1212.

[13] E.E. Brumbaugh and G.K. Ackers, J. Biol. Chem. 243 (1968) 6315.

[14] H.S. Warshaw and G.K. Ackers, Anal. Biochem. 42 (1971) 405.

[15] E.E. Brumbaugh and G.K. Ackers, Anal. Biochem. 41 (1971) 543.

[16] G.A. Morton, Appl. Opt. 7 (1968) 1.

[17] H.V. Malmstadt, M.S. Franklin and G. Horlick, Anal. Chem. 44 (1972) 63A.

[18] Y. Beers, Introduction to the Theory of Error (Addison–Wesley, Reading, Mass., 1957).

[19] G.K. Ackers and H.R. Halvorson, Proc. Natl. Acad. Sci. 71 (1974) 4312.

[20] S.H.C. Ip, M.L. Johnson and G.K. Ackers, Biochemistry, in press.